



A deep learning radiomics model may help to improve the prediction performance of preoperative grading in meningioma

Liping Yang¹ · Panpan Xu¹ · Ying Zhang¹ · Nan Cui¹ · Menglu Wang¹ · Mengye Peng¹ · Chao Gao² · Tianzuo Wang³ 

Received: 1 October 2021 / Accepted: 4 January 2022 / Published online: 17 January 2022
© The Author(s), under exclusive licence to Springer-Verlag GmbH Germany, part of Springer Nature 2022

Abstract

Purpose This study aimed to investigate the clinical usefulness of the enhanced-T1WI-based deep learning radiomics model (DLRM) in differentiating low- and high-grade meningiomas.

Methods A total of 132 patients with pathologically confirmed meningiomas were consecutively enrolled (105 in the training cohort and 27 in the test cohort). Radiomics features and deep learning features were extracted from T1 weighted images (T1WI) (both axial and sagittal) and the maximum slice of the axial tumor lesion, respectively. Then, the synthetic minority oversampling technique (SMOTE) was utilized to balance the sample numbers. The optimal discriminative features were selected for model building. LightGBM algorithm was used to develop DLRM by a combination of radiomics features and deep learning features. For comparison, a radiomics model (RM) and a deep learning model (DLM) were constructed using a similar method as well. Differentiating efficacy was determined by using the receiver operating characteristic (ROC) analysis.

Results A total of 15 features were selected to construct the DLRM with SMOTE, which showed good discrimination performance in both the training and test cohorts. The DLRM outperformed RM and DLM for differentiating low- and high-grade meningiomas (training AUC: 0.988 vs. 0.980 vs. 0.892; test AUC: 0.935 vs. 0.918 vs. 0.718). The accuracy, sensitivity, and specificity of the DLRM with SMOTE were 0.926, 0.900, and 0.924 in the test cohort, respectively.

Conclusion The DLRM with SMOTE based on enhanced T1WI images has favorable performance for noninvasively individualized prediction of meningioma grades, which exhibited favorable clinical usefulness superior over the radiomics features.

Keywords Meningiomas · Magnetic resonance imaging (MRI) · Radiomics · Deep learning

Introduction

Meningiomas are the most common primary extra-axial neoplasms in adults, accounting for 36.7% of all central nervous system tumors in the USA [1, 2]. The World Health Organization (WHO) classification is one of the major prognostic factors and was applied to tailor treatment strategies [3–6]. According to the WHO classification system, meningiomas can be classified into three grades: grade I (benign), grade II (atypical), and grade III (anaplastic) [7]. In general,

low-grade (grade I) meningiomas were treated following an indolent clinical course, and complete surgical resection can achieve favorable survival outcomes [8]. By contrast, high-grade meningiomas (grade II, grade III) tend to exhibit more aggressive biological behavior and poorer clinical prognosis, with relatively high 5-year recurrence rates of 50 to 90% [9]. For individuals with grade I meningiomas, surgical resection or radiosurgery alone is usually recommended in clinical practice, and adjuvant radiotherapy is only necessary for residual tumor tissue. However, for highly aggressive grade II and grade III meningiomas, adjuvant radiotherapy may be necessary and beneficial even after complete resection [10]. Furthermore, for those patients with high-grade meningiomas, additional treatment strategies such as radiotherapy and/or chemotherapy are required frequently [6]. Therefore, accurately grading prior to surgery is critically important for patients with meningiomas in clinical settings [11].

Presently, the noninvasive imaging technique available for assessment of meningiomas is mainly MRI because of

✉ Tianzuo Wang
agntwz@126.com

¹ PET-CT/MR Department, Harbin Medical University Cancer Hospital, Harbin, China

² Medical Imaging Department, The Fourth Affiliated Hospital of Harbin Medical University, Harbin, China

³ Medical Imaging Department, The Second Affiliated Hospital of Harbin Medical University, Harbin, China

relatively high convenience and soft-tissue resolution, as well as providing the tumor dynamic blood supply information [6–10]. Although some researchers have demonstrated that MRI could provide valuable information for the evaluation of meningiomas, the radiological performance of different grades is largely overlapped, which could lead to misdiagnosis and inappropriate treatment strategies [12–14].

Machine learning (ML), an intersection of statistics and computer science, is a branch of artificial intelligence as it enables the extraction of meaningful patterns from examples, which is a component of human intelligence [15]. Over the last decade, it has been successfully applied in the field of radiology, particularly in automatically detecting disease and discriminating tumors [16]. Recently, some studies demonstrated that ML-based on MRI was a promising tool in grading meningiomas [17]. However, few radiomics studies combined with deep learning features were extracted using a pretrained convolutional neural network (CNN). Thus, we decided to evaluate the performance of a DLRM based on enhanced-T1WI images for preoperative differentiating low- and high-grade meningiomas and compare with that of RM and DLM.

Materials and methods

Study population

The research protocol was reviewed, approved, and overseen by the review board of *BLINDED 1*. The informed consent was waived due to the retrospective nature. Specific inclusion criteria were listed as follows: (1) pathologically confirmed intracranial meningiomas and histopathological grade of meningiomas were determined according to the guidelines of WHO criteria [18]; (2) previously untreated solitary primary tumor before MRI scans; (3) available preoperative brain MRI scans including axial and sagittal enhanced T1WI prior to surgical resection. The exclusion criteria were as follows: (1) unsatisfactory image quality, such as artifacts or incomplete tumor display (only partial tumor was scanned); (2) a history of relevant treatment (including radiotherapy or surgery) before MRI scans; (3) multiple lesions. All enrolled patients were randomly divided into training cohorts and test cohorts according to a ratio of 8:2. The test cohort was only used for testing the performance of the models. The flowchart of patient selection is shown in Supplementary Fig. 1.

Image acquisition

The examinations were performed by using an MRI 3.0T scanner (Discovery MR750w, GE Medical Systems). All MRI scans were completed within 2 weeks prior to surgical

resection. The unenhanced scanning sequences included sagittal T1WI, axial T1WI, and axial T2WI. Enhanced scanning sequences included axial and sagittal T1WI. Specific T1WI sequence parameters were displayed as follows: repetition time [TR] 500 ms, echo time [TE] 10 ms, matrix size 256 × 256, slice thickness 5 mm, and field of view [FOV] 230 × 230 mm. T2WI images were acquired using the following scan parameters: TR 5200 ms, TE 95 ms, matrix size 256 × 256, slice thickness 5 mm, and FOV 23 cm. All enhanced T1WI images were acquired after administration of gadopentetate dimeglumine (0.1 ml/kg).

Image preprocessing

The processing of developing DLRM with synthetic minority oversampling technique (SMOTE) is presented in Fig. 1. Before data analysis, image preprocessing was performed, including image normalization, resampling, and N4 bias field correction. Unwanted low-frequency intensity nonuniformity was removed by implementing the N4 bias correction using SimpleITK software (version 2.0, <https://www.simpleitk.org/>) [19]. After that, the images were further normalized in order to reduce brightness and contrast variations. For the radiomics feature, the normalization option on the pyradiomics software (version 3.0, <https://pyradiomics.readthedocs.io/en/latest/>) is used, which enabled the normalization of image intensity values prior to feeding them into the extraction pipeline. Normalization operation is based on all gray values contained within the images, not just those defined by the ROI in the mask. For the deep learning feature, we used the torchvision package (version 0.9, <https://pytorch.org/vision/stable/index.html>) to normalize the images before feeding them into pretrained ResNet. In addition, all MRI images were resampled to a uniform voxel size of 1 mm × 1 mm × 1 mm for subsequent image processing.

Tumor segmentation

For obtaining ROI, manual segmentation was performed on the meningioma images. The enhanced tumor images were imported into ITK-SNAP (version 3.8.0, <https://www.itknap.org/>) with the tumor lesion areas manually delineated by two radiologists (both of who have more than 10-year practicing experience in brain MRI) blinded to the pathological results. The maximum area slice of the tumor lesion was selected and delineated, and the adjacent bone invasion was excluded as much as possible. As for deep learning features extraction, the maximum area slice of the tumor was chosen for delineating, and the adjacent bone invasion was excluded. Then, the tumor was cropped using a rectangle bounding box and resized into 299 × 299 pixels. The tumor segmentation process is presented in Fig. 2.

Fig. 1 Overview of the radiomics analysis framework for the differentiation of meningiomas. Image preprocessing was performed prior to data analysis. Features were extracted and then combined with feature reproducibility for feature selection. Prediction models were constructed based on LightGBM algorithm for meningioma differentiation. Finally, models were evaluated and tested

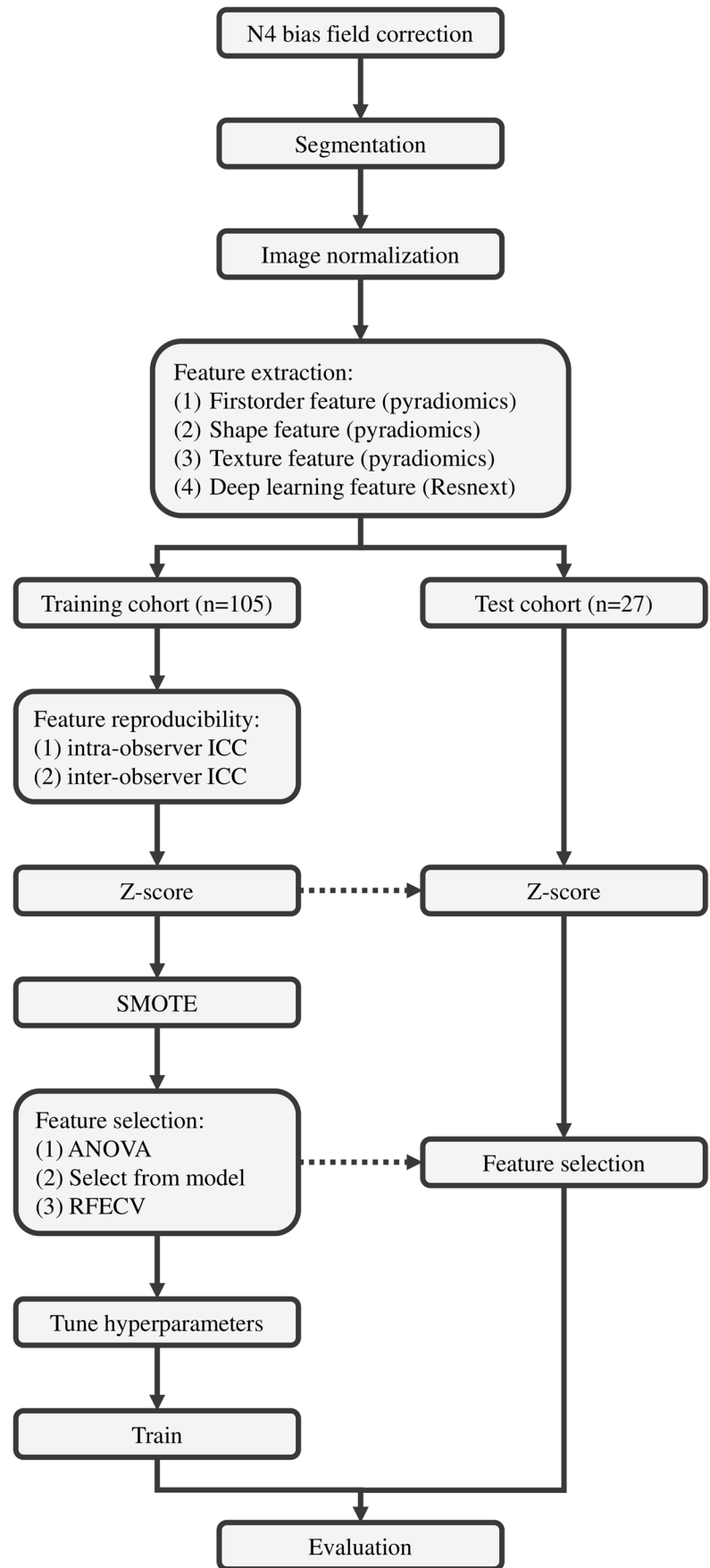
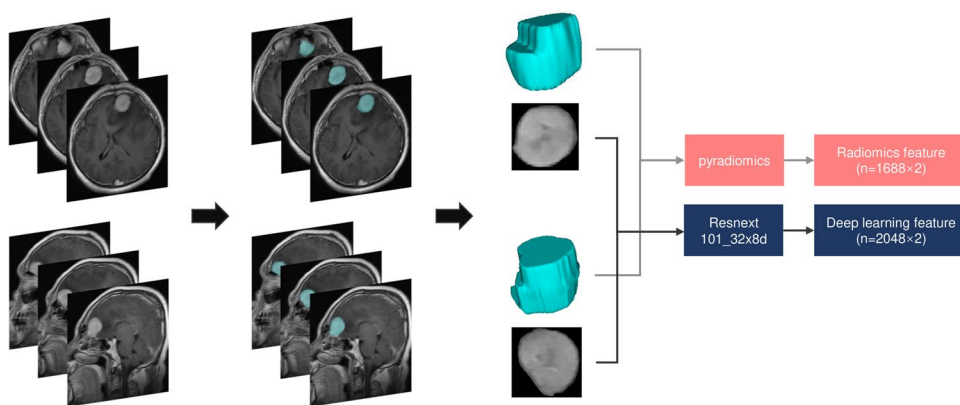


Fig. 2 The tumor segmentation process



Feature extraction

Radiomics features were extracted by using pyradiomics (version 3.0, <https://pyradiomics.readthedocs.io/>) [20]. For each patient, a total of 1688 radiomics features could be extracted from each sequence, including seven categories: first-order, shape, gray-level cooccurrence matrix (GLCM), gray-level dependence matrix (GLDM), gray-level size zone matrix (GLSZM), gray-level run-length matrix (GLRLM), and neighboring gray-tone difference matrix (NGTDM). All filters were enabled. To obtain deep learning features, we used the pretrained Resnext101_32x8d without the Softmax layer of PyTorch (version 1.8.1, <https://pytorch.org/>) as a feature extractor, which could yield 2048 deep learning features after feeding an image. The naming method of deep learning features was as follows: DLF_number_sequence. Finally, a total of 7472 features ($1688 \times 2 + 2048 \times 2$) could be extracted from axial and sagittal enhanced T1WI images of each meningioma.

Feature reproducibility

Intra- and interobserver reproducibility of feature extraction was assessed by calculating the intra- and interclass correlation coefficients (ICCs). For all cases in the training cohort, radiologists A and B extracted the features independently, and radiologist A reextracted features 2 weeks later. Radiomics features with ICC lower than 0.90 were not used to further analysis. The second segmentation results by radiologist A were finally chosen.

Data analysis

Data analysis, including data preprocessing, feature selection, and model development and evaluation, was performed by using the scikit-learn package (version 0.23.2, [https://](https://scikit-learn.org/)

scikit-learn.org/) in Python (version 3.8, <https://www.python.org/>) [21].

Before feature selection, the mean and standard deviation of each feature in the training cohort were calculated one by one, and the values of each feature were normalized with *Z*-score ($Z = (x - \text{mean}) / \text{standard deviation}$). Subsequently, SMOTE was adopted due to the imbalance number of low- and high-grade meningiomas [22].

A three-step feature selection was applied to find optimal feature combinations. First of all, we calculated the ANOVA *p*-value between label and features for classification tasks and removed the features with $p > 0.05$. Next, the feature importance of each feature was calculated by using the LightGBM algorithm, and the features ranked in the top 20 were retained [23]. Finally, recursive feature elimination with 5-fold cross-validation (RFECV) was performed to select the most effective combination of the features according to the area under the curve (AUC) mean. To obtain optimal hyperparameters, a grid search with 5-fold cross-validation was implemented.

Models' development and diagnostic performance assessment

We constructed a DLRM using LightGBM algorithm by combining two categories of features [24]. Considering the performance comparison, we also applied a similar method to construct the other five models. All predictive models were trained by the training cohort and then tested using the test cohort. The flowchart of developing models is shown in Supplementary Fig. 2. The predictive performance of the developed models was assessed using the ROC curve. The accuracy, sensitivity, and specificity were calculated based on the independent test cohort.

Results

Patients' characteristics

Patients with multiple lesions ($n = 9$), a history of treatment before MRI scans ($n = 8$), and substandard image quality, such as artifacts or incomplete tumor display (only partial tumor was scanned) ($n = 4$) were excluded. Finally, a total of 132 patients with meningiomas from January 2017 to December 2020 were retrospectively reviewed in our study, composed of 39 males and 93 females (ranging from 34 to 72 years old, median 56). Forty-eight patients were assigned to high-grade meningiomas, and 84 patients were confirmed with low-grade meningiomas. Next, they were randomly divided into training cohorts ($n = 105$) and test cohorts ($n = 27$) according to the 8:2 ratio.

Feature screening

The intra-observer ICC ranged from -0.766 to 1 , and inter-observer ICC was ranged from -0.936 to 1 . A total of 7472 features were extracted for each patient, and 4833 features were excluded due to poor reproducibility (ICC range: -0.936 to 0.899). All the extracted features are listed in Supplementary Material 1.

Then, 341 features were kept after removing features with $p < 0.05$. The top 20 features ranked by the LightGBM algorithm were entered in RFECV to select the most effective combination of the features. At last, a total of 15 features, including 12 radiomics features and 3 deep learning features,

were selected to construct the DLRM using SMOTE. The selected features and corresponding importance are displayed in Fig. 3. The heat map of the selected features is shown in Fig. 4. The features selected for developing RM and DLM were listed in Supplementary Material 2.

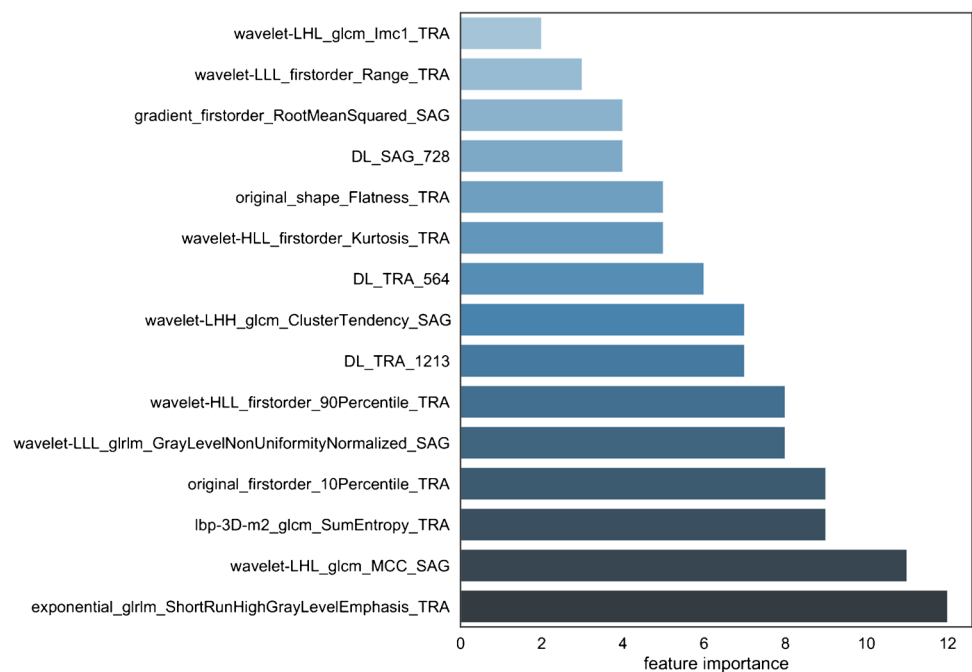
Predictive performance of the radiomics features

The test cohort was used to evaluate the performance in differentiating low- and high-grade meningiomas. The AUC, accuracy, sensitivity, and specificity of the DLRM were 0.912, 0.889, 1.000, and 0.824 in the test cohort, respectively. The performance of the DLRM outperformed that of the RM and the DLM both in the training and test cohorts (training AUC: 0.950, 0.839; test AUC: 0.888, 0.656). The models using SMOTE showed better performance. After the adoption of SMOTE, the AUC, accuracy, sensitivity, and specificity of the DLRM were 0.935, 0.926, 0.900, and 0.924 in the test cohort, respectively, which is still superior to the performance of the RM and the DLM both in the training and test cohort (training AUC: 0.980, 0.892; test AUC: 0.918, 0.718). ROC curves are shown in Fig. 5a and b. All diagnostic performance parameters are listed in Table 1.

Discussion

The meningioma grade prediction was a crucial determinant for tumor recurrence and the patient's overall survival. For patients with meningiomas, the clinical prognosis of different pathological grades is significantly different such

Fig. 3 The selected features and corresponding importance



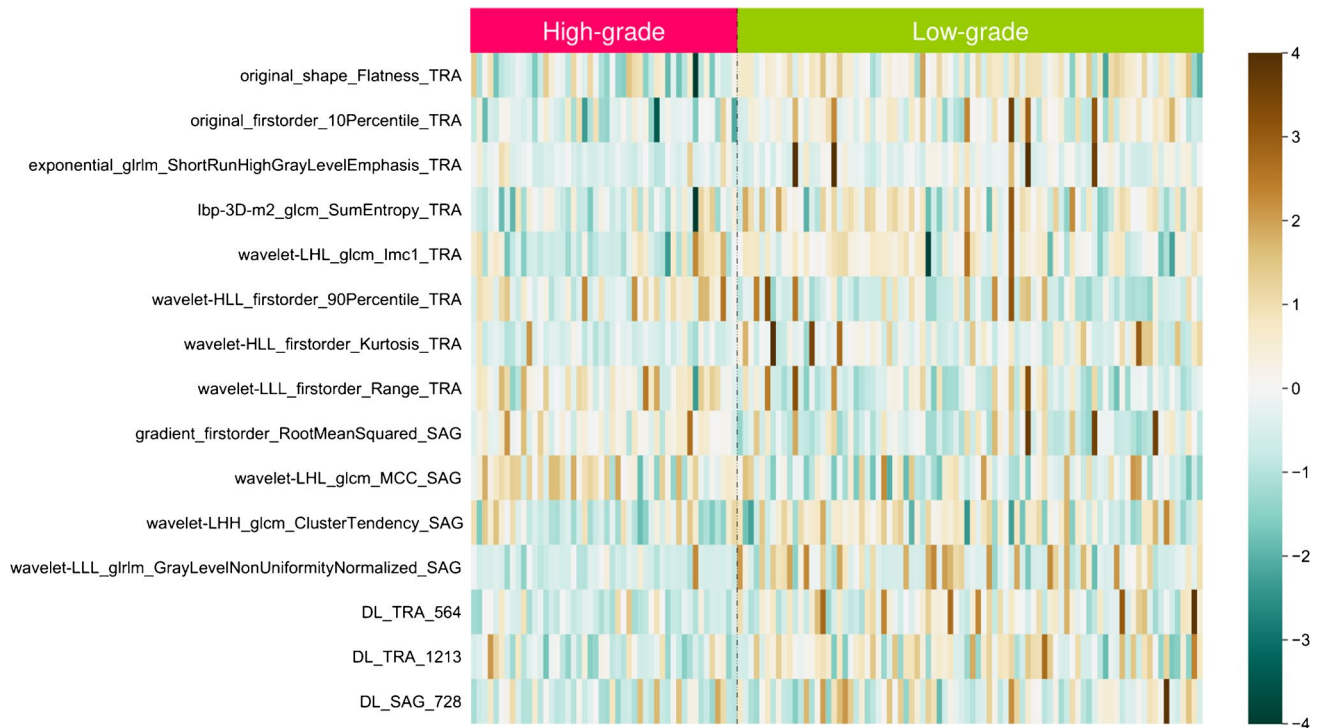
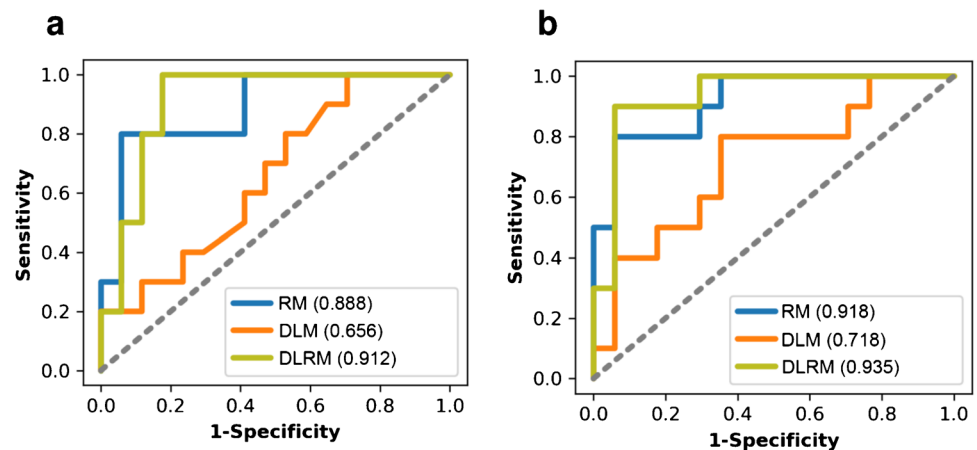


Fig. 4 The heat map of the selected features.

Fig. 5 ROC curves of test cohort



that higher pathological grades of meningiomas tend to be with a higher recurrence rate (I: 7–25%; II: 29–52%; III: 50–94%) [25]. Therefore, given marked differences in treatment strategy and survival outcome, accurate and noninvasive evaluation of pathological tumor grade prior to surgery is of vital significance to assist in developing a personalized therapeutic schedule. In the present study, we constructed a DLRM based on axial and sagittal enhanced T1WI images, which showed favorable performance for differentiating low- and high-grade meningiomas. By contrast, the DLRM-based model demonstrated better performance than RM and DLM-based models. The AUC for the DLRM-based model was

0.988 in the training cohort, whereas the RM-based model was 0.980, and the DLM-based model was 0.892. The AUC for the DLRM-based model was 0.935 in the test cohort, whereas the RM-based model was 0.918, and the DLM-based model was 0.718. Generally, the performance in the test set should be slightly worse, as it is unlikely that no matter what model performs best on the training set would perform equally well on every other unseen set of data. In addition, we guessed that the performance of our model in the test cohort was attenuated by the limited population size and imbalanced proportions between the low-grade and high-grade meningioma patients. Further studies with

Table 1 Performance of different models in the training and test cohort

Model		Training	Test			
		AUC	AUC	Sensitivity	Specificity	Accuracy
RM	None	0.950	0.888	0.800	0.941	0.889
	SMOTE	0.980	0.918	0.800	0.941	0.889
DLM	None	0.839	0.656	1.000	0.294	0.556
	SMOTE	0.892	0.718	0.800	0.647	0.704
DLRM	None	0.973	0.912	1.00	0.824	0.889
	SMOTE	0.988	0.935	0.900	0.924	0.926

the inclusion of more data are required to strengthen these findings.

Meningioma grading is crucial because it aids in treatment planning [26]. MRI is the first choice for the diagnosis and preoperative assessment of meningiomas [6, 27]. Nevertheless, the value of conventional sequences is limited for differentiating the grades of meningiomas, and controversial results have been reported for apparent diffusion coefficient values [12, 28]. It is well known that the presence of intratumoral edema, hemorrhage, and necrosis produce heterogeneous tumor parenchyma, which is closely related to the high aggressiveness of the tumor. However, those semantic features are generally highly subjective through visual evaluation by the radiologists, thereby resulting in great interobserver variability in clinical practice. In contrast, radiomics as a promising approach was applied in noninvasive meningioma grading and demonstrated favorable performance [17]. Lorenzo et al. summarized eight related radiomics studies, where the pooled AUC of studies employed a test cohort achieved 0.84 (95% confidence intervals [CI] = 0.78–0.90), suggesting that radiomics could serve as an effective tool in grading meningiomas [17]. Thus, the present study investigated the clinical usefulness of machine learning-based radiomics analysis in differentiating low- and high-grade meningiomas.

Currently, various machine learning algorithms have been applied to radiomics analysis. Such as random forest, decision tree (DT), and so on. As a novel and advanced Gradient-Boosting Decision Tree (GBDT) algorithm, LightGBM was proposed in 2017 by Microsoft Research Asia. LightGBM is a distributed and high-performance gradient lifting framework based on a DT machine learning algorithm. The advantages of the LightGBM algorithm include ingredient-based one-side sampling and exclusive feature bundling, which were used to deal with the huge number of data samples and a massive amount of radiomics features. Additionally, LightGBM demonstrates faster data training speed with a lower memory cost in comparison with traditional boosting algorithms. Thus, LightGBM enables to realize the extraction of high-throughput data [29].

In our study, we finally extracted a sum of 3376 radiomics features from each patient, which consisted of more

advanced high-order features not just the inclusion of the first-order features. The entropy belongs to the GLCM feature pool, which essentially reflects the intensity of the spatial distribution. Specifically, the larger entropy value represents the greater tumor heterogeneity. At the same time, the GLSZM describes the uniformity of the tumor texture. In general, high-grade meningiomas are featured by a larger proportion of tissue disruption and thus a higher heterogeneity of the distribution of cells in the tumor lesions compared with low-grade lesions [30]. These radiomics features can be used to reflect the spatial heterogeneity of meningiomas of different pathological grades. Based on this fact, we successfully developed a RM based on enhanced T1WI images for grading meningiomas, achieving an AUC of 0.918 in the test cohort.

Contrast-enhanced T1WI images before surgery analyzed in our study could be attributed to the following reasons: (1) a series of previously reported works that predict the pathological grade of meningiomas based on presurgical MRI images were mainly focused on these imaging sequences; (2) the deep learning features derived from contrast-enhanced T1WI images have recently demonstrated good discrimination performance in both the primary and test cohorts, with an AUC of 0.811 in the test cohort [11]. It is well-known that most meningiomas manifest as a marked enhancement on enhanced T1WI images due to abundant blood supply. Thus, the tumor boundaries can be clearly displayed. A series of previously reported works that predict the pathological grade of meningiomas based on presurgical MRI images were mainly focused on these imaging sequences in order to obtain more robust results. Furthermore, the diagnostic performance comparison between the T1WI and T2WI sequences in a previous study draws the conclusion that a predictive model cohort up with an enhanced T1WI sequence shows a better differentiating ability of meningiomas, so we only outline volume of interest on the enhanced T1WI images [27, 31, 32].

The clinical usefulness in determining the pathological grade of meningiomas using enhanced T1WI images has been investigated by several researchers, with discrepant results. The study conducted by Laukamp et al. reported an AUC of 0.76 in the differentiation between low-grade

and high-grade meningiomas. However, firstly, a previous study was carried out on a relatively small sample size (71 patients). Secondly, only shape and texture features were extracted from conventional enhanced T1WI images; advanced radiomics features were not obtained for technical reasons [31]. In contrast, the AUC of radiomics features was 0.950 in the current study, which demonstrated a higher diagnostic efficacy. The current study was applied a relatively larger sample size (132 cases), higher-order features (such as Gy level co-occurrence matrix (GLCM) feature and neighborhood gray-tone difference matrix (NGTDM) feature), as well as a more advanced radiomics analysis approach. Another previous study reported that radiomics feature-based machine learning classifiers of enhanced T1WI images are useful for differentiating meningioma grades. However, the study population was insufficient with analyses of just the largest dimension of the tumor on the enhanced T1 sequence instead of the analysis of the whole tumor, and the ignorance of data imbalance has to be admitted. It is inevitable that the existence of the data imbalance in meningioma grading resulted from the relatively low incidence of high-grade meningiomas, which has an adverse effect on the fitting of radiomics classification models [33]. In the present study, the state-of-the-art subsampling technique was recommended as a suitable strategy to remedy this defect, and the predictive performance was improved by using SMOTE.

Conventional machine-learning techniques show limited capabilities to process natural data in their raw form. The construction of a pattern-recognition system requires careful engineering and rich knowledge to design a feature extractor that enables the transformation from the raw data into a feature vector [34]. The deep learning approach is a representation learning method that allows a machine to be fed with raw data and to discover the representations needed for classification. DCNNs automatically utilized filters to create radiomics feature maps describing the distribution of such features derived from medical. An increased number of clinical applications of DCNNs in neuroradiology have been reported [35].

A previous study conducted by Zhang et al. designed a deep learning algorithm to predict meningioma grade. For meningioma grade classification, the prediction accuracy in the test cohort was 81.52%, demonstrating a better diagnostic performance in comparison with our results (81.52%) [36]. Banzato et al. studied 117 meningioma-affected cases and reported that DCNNs could accurately discriminate between benign and atypical/anaplastic meningiomas from ADC maps but not from enhanced T1WI images. The discriminating accuracy of both DCNNs on postcontrast T1WI images was low, with Inception-v3 displaying an AUC of 0.68 (95% CI, 0.59–0.76) and AlexNet displaying an AUC of 0.55 (95% CI, 0.45–0.64) [37]. In the present study, we

reported an AUC of 0.839 in the training cohort and an AUC of 0.656 in the test cohort. The slight inconsistency between the above findings and our own results is probably because of the different sample sizes and MRI scanners with varying field strength (1.5T and 3.0T) and vendors.

In order to further obtain robust results, we investigated the additional value of DLRM in grading meningiomas. Our data suggested that deep learning radiomics-based feature analysis yielded strong classification performances for meningioma grading. Recently, Zhu et al. combined radiomics features with deep learning features to construct a comprehensive model for grading meningiomas, the AUC of which was 0.814 in the test cohort [11]. In the present study, ANOVA was firstly used to select the top ten important features, then the RFECV was performed to the most discriminating features. We retained features with greater contribution, which were then utilized to develop a DLRM. Subsequently, the verification cohort was substituted into the prediction model for further testing. The final results confirmed that the AUC of the verification cohort was as high as 0.912, thus demonstrating that the DLRM is reliable. Presumably, it was because that we added the features extracted from sagittal images and used pretrained Resnext101_32x8d as feature extractor, which was one of the state-of-the-art CNN models, achieving an accuracy of 0.854 in the ImageNet dataset [38]. Moreover, the radiomics features were extracted from all lesion slices instead of three consecutive slices, and thus they could reflect tumor heterogeneity comprehensively. All of which were able to make us obtain more valuable information.

This study has several limitations: (1) potential selection bias might exist because of the retrospective nature. (2) We only outlined the VOIs in tumor parenchyma. Thus, the potential significance of peritumoral edema areas for the grading of meningiomas should be explored in the near future. (3) The study sample size was limited, and a larger number of cases should be included in a subsequent study, and external test data also are needed for further validation.

In summary, this study demonstrates that the application of DLR analysis based on contrast-enhanced T1WI images provides great clinical usefulness in differentiation between high-grade and low-grade meningiomas. In addition, further investigation, including a much larger number of populations from multicenter, should be carried out to better expand the generalization ability of this method.

Conclusion

In summary, the deep learning radiomics model based on enhanced T1WI images has favorable performance for differentiating low- and high-grade meningiomas, and the

addition of deep learning features is able to improve the performance of the radiomics model. Besides, additional studies with high methodological quality are still required to validate our results.

Supplementary Information The online version contains supplementary material available at <https://doi.org/10.1007/s00234-022-02894-0>.

Acknowledgments The authors would like to especially thank Professor Thelma R. Gower for her assistance with the preparation of this manuscript.

Authors' contributions Substantial contributions to the conception of the work: Liping Yang, Panpan Xu, Ying Zhang, and Tianzuo Wang. Substantial contributions to the acquisition of data: all authors. Substantial contributions to the analysis of data: Liping Yang, Panpan Xu, Ying Zhang, Nan Cui, Menglu Wang, Mengye Peng, Chao Gao, and Tianzuo Wang. Substantial contributions to interpretation of data for the work: Liping Yang, Panpan Xu, Ying Zhang, Nan Cui, Menglu Wang, Mengye Peng, Chao Gao, and Tianzuo Wang. Drafting the work or revising it critically for important intellectual content: all authors. Final approval of the version to be published: all authors.

Funding This paper is supported by the Haiyan Funding [grant number JJQN2019-23 to LY]. The funders had no role in study design, data collection and analysis, decision to publish, or preparation of the manuscript.

Availability of data and material Research data are not available for public access due to patient privacy concerns but can be obtained from the corresponding author on reasonable request approved by the institutional review boards of all participating institutions.

Code availability Not applicable.

Compliance with ethical standards

Conflicts of interest The authors declare that they have no conflicts of interest.

Ethical approval All procedures performed in studies involving human participants were in accordance with the ethical standards of the institutional research committee of the Harbin Medical University Cancer Hospital.

Consent to participate For this type of retrospective study, formal consent is not required.

Consent for publication All authors agree to the publication of this paper.

References

- Wiemels J, Wrensch M, Claus EB (2010) Epidemiology and etiology of meningioma. *J Neuro-Oncol* 99:307–314
- Alexandru D, Glantz MJ, Kim L et al (2011) Pulmonary metastases in patients with recurrent, treatment-resistant meningioma: prognosis and identification by Indium-octreotide imaging. *Cancer* 117:4506–4511
- Spille D, Adeli A, Sporns P et al (2021) Predicting the risk of postoperative recurrence and high-grade histology in patients with intracranial meningiomas using routine preoperative MRI. *Neurosurg Rev* 44:1109–1117
- Lam Shin Cheung V, Kim A, Sahgal A et al (2018) Meningioma recurrence rates following treatment: a systematic analysis. *J Neuro-Oncol* 136:351–361
- Biczok A, Jungk C, Egensperger R et al (2019) Microscopic brain invasion in meningiomas previously classified as WHO grade I is not associated with patient outcome. *J Neuro-Oncol* 145:469–477
- Goldbrunner R, Minniti G, Preusser M et al (2016) EANO guidelines for the diagnosis and treatment of meningiomas. *Lancet Oncol* 17:e383–e391
- Willis J, Smith C, Ironside JW et al (2005) The accuracy of meningioma grading: a 10-year retrospective audit. *Neuropathol Appl Neurobiol* 31:141–149
- Bertero L, Dalla Dea G, Osella-Abate S et al (2019) Prognostic characterization of higher-grade meningiomas: a histopathological score to predict progression and outcome. *J Neuropathol Exp Neurol* 78:248–256
- Ly KI, Hamilton SR, Rostomily RC et al (2015) Improvement in visual fields after treatment of intracranial meningioma with bevacizumab. *J Neuroophthalmol* 35:382–386
- Buerki RA, Horbinski CM, Kruser T et al (2018) An overview of meningiomas. *Future Oncol* 14:2161–2177
- Zhu Y, Man C, Gong L et al (2019) A deep learning radiomics model for preoperative grading in meningioma. *Eur J Radiol* 116:128–134
- Huang RY, Bi WL, Griffith B et al (2019) Imaging and diagnostic advances for intracranial meningiomas. *Neuro-Oncology* 21:i44–i61
- Spille D, Sporns P, Heß K et al (2019) Prediction of high-grade histology and recurrence in meningiomas using routine preoperative magnetic resonance imaging: a systematic review. *World Neurosurg* 128:174–181
- Ke C, Chen H, Lv X et al (2020) Differentiation between benign and nonbenign meningiomas by using texture analysis from multiparametric MRI. *J Magn Reson Imaging* 51:1810–1820
- Radakovich N, Nagy M, Nazha A (2020) Machine learning in haematological malignancies. *Lancet Haematol* 7:e541–e550
- Martin Noguero T, Paulano-Godino F, Martin-Valdivia MT et al (2019) Strengths, weaknesses, opportunities, and threats analysis of artificial intelligence and machine learning applications in radiology. *J Am Coll Radiol* 16:1239–1247
- Ugga L, Perillo T, Cuocolo R et al (2021) Meningioma MRI radiomics and machine learning: systematic review, quality score assessment, and meta-analysis. *Neuroradiology* 63:1293–1304
- Wen PY, Huse JT (2017) 2016 World Health Organization classification of central nervous system tumors. *Continuum (Minneapolis)* 23:1531–1547
- Tustison NJ, Avants BB, Cook PA et al (2010) N4ITK: improved N3 bias correction. *IEEE Trans Med Imaging* 29:1310–1320
- van Griethuysen JJM, Fedorov A, Parmar C et al (2017) Computational radiomics system to decode the radiographic phenotype. *Cancer Res* 77:e104–e107
- Pedregosa F, Varoquaux G, Gramfort A et al (2012) Scikit-learn: machine learning in Python
- Nakamura M, Kajiwara Y, Otsuka A et al (2013) LVQ-SMOTE - Learning Vector Quantization based Synthetic Minority Over-sampling Technique for biomedical data. *BioData Min* 6:16
- Nie P, Wang N, Pang J et al (2021) CT-based radiomics nomogram: a potential tool for differentiating hepatocellular adenoma from hepatocellular carcinoma in the noncirrhotic liver. *Acad Radiol* 28:799–807

24. Meng Q (2018) LightGBM: a highly efficient gradient boosting decision tree
25. Kawahara Y, Nakada M, Hayashi Y et al (2012) Prediction of high-grade meningioma by preoperative MRI assessment. *J Neuro-Oncol* 108:147–152
26. Apra C, Peyre M, Kalamarides M (2018) Current treatment options for meningioma. *Expert Rev Neurother* 18:241–249
27. Hu J, Zhao Y, Li M et al (2020) Machine learning-based radiomics analysis in predicting the meningioma grade using multiparametric MRI. *Eur J Radiol* 131:109251
28. Bohara M, Nakajo M, Kamimura K et al (2020) Histological grade of meningioma: prediction by intravoxel incoherent motion histogram parameters. *Acad Radiol* 27:342–353
29. Zhang J, Mucs D, Norinder U et al (2019) LightGBM: an effective and scalable algorithm for prediction of chemical toxicity-application to the Tox21 and mutagenicity data sets. *J Chem Inf Model* 2019
30. Vranes V, Vujasinovic T, Rajkovic N et al (2020) Analysis of spatial distribution and prognostic value of different pan cytokeratin immunostaining intensities in breast tumor tissue sections. *Int J Mol Sci* 21
31. Laukamp KR, Shakirin G, Baessler B et al (2019) Accuracy of radiomics-based feature analysis on multiparametric magnetic resonance images for noninvasive meningioma grading. *World Neurosurg* 132:e366–e390
32. Hamerla G, Meyer HJ, Schob S et al (2019) Comparison of machine learning classifiers for differentiation of grade 1 from higher gradings in meningioma: a multicenter radiomics study. *Magn Reson Imaging* 63:244–249
33. Han Y, Wang T, Wu P et al (2021) Meningiomas: preoperative predictive histopathological grading based on radiomics of MRI. *Magn Reson Imaging* 77:36–43
34. Agarwalla S, Sarma KK (2016) Machine learning based sample extraction for automatic speech recognition using dialectal Assamese speech. *Neural Netw* 78:97–111
35. Jing Y, Bian Y, Hu Z et al (2018) Deep learning for drug design: an artificial intelligence paradigm for drug discovery in the Big Data Era. *AAPS J* 20:58
36. Zhang H, Mo J, Jiang H et al (2021) Deep learning model for the automated detection and histopathological prediction of meningioma. *Neuroinformatics* 19:393–402
37. Banzato T, Causin F, Della Puppa A et al (2019) Accuracy of deep learning to differentiate the histopathological grading of meningiomas on MR images: a preliminary study. *J Magn Reson Imaging* 50:1152–1159
38. Mlynarski P, Delingette H, Criminisi A, et al (2018) 3D convolutional neural networks for tumor segmentation using long-range 2D context.

Publisher's note Springer Nature remains neutral with regard to jurisdictional claims in published maps and institutional affiliations.